INTERNATIONAL MONETARY FUND

# Building Macroeconomic Resilience to Natural Disasters and Persistent Temperature Changes: The Case of Peru

Zamid Aligishiev and Daria Kolpakova

WP/25/144



**2025**
JUL

WORKING PAPER

 WP/25/144

**IMF Working Paper**
WHD

# Building Macroeconomic Resilience to Natural Disasters and Persistent Temperature Changes: The Case of Peru

**Prepared by Zamid Aligishiev and Daria Kolpakova***

Authorized for distribution by Sònia Muñoz
July 2025



**ABSTRACT:** Peru is highly exposed to periodic El Niño Costero events, which impair production in the country's fishing, agriculture, and construction sectors, as well as inflict sizeable damages to physical assets. Moreover, rising average temperatures are expected to diminish productivity in agriculture, fisheries, and energy. Without efforts to strengthen its adaptive capacity, the country remains highly vulnerable to such acute and chronic physical risks in the long term. This paper combines a Markov-switching DSGE model with empirical estimates of losses from such risks to conduct a scenario analysis of their macro-fiscal implications. We find that cumulative income losses could reach up to 18.6 percent by 2050 and 50.6 percent by 2100. The analysis further shows that scaling up investments in structural resilience and adaptation can partially mitigate these losses—raising output by up to 12.3 percent by 2050 and 31 percent by 2100—while also generating long-term fiscal savings.

**RECOMMENDED CITATION:** Aligishiev and Kolpakova. 2025. Building Macroeconomic Resilience to Natural Disasters and Persistent Temperature Changes: The Case of Peru. Working Paper WP/25/144. International Monetary Fund, Washington D.C.

| | |
|---|---|
| JEL Classification Numbers: | Q54, H54, O54 |
| Keywords: | El Niño, Weather shocks, Structural resilience, Acute physical risk, Chronic physical risk. |
| Author's E-Mail Address: | ZAligishiev@imf.org, DKolpakova@imf.org |

* The authors are grateful to Sònia Muñoz, Matthieu Bellon, Emilio Fernández Corugedo, George Cui, Pedro Juarros, Emanuele Massetti, Gregor Schwerhoff, Filippos Tagklis, and the staff of the Ministerio del Ambiente for their invaluable suggestions and comments, as well as to the workshop participants at the Banco Central de Reserva del Perú for their insightful discussions.

WORKING PAPERS

# Building Macroeconomic Resilience to Natural Disasters and Persistent Temperature Changes: The Case of Peru

Prepared by Zamid Aligishiev and Daria Kolpakova[1]

[1] The authors are grateful to Sònia Muñoz, Matthieu Bellon, Emilio Fernández Corugedo, George Cui, Pedro Juarros, Emanuele Massetti, Gregor Schwerhoff, Filippos Tagklis, and the staff of the Ministerio del Ambiente for their invaluable suggestions and comments, as well as to the workshop participants at the Banco Central de Reserva del Perú for their insightful discussions.

# Contents



# List of Figures

## List of Tables

# 1 Introduction

Between 2003 and 2019, Peru experienced over 61,000 emergencies linked to natural hazards (World Bank, 2022). The acute physical risk profile of the country is dominated by floods, landslides, droughts, and storms. These natural hazards weigh heavily on socio-economic outcomes and constitute recurring fiscal costs as authorities rebuild damaged infrastructure and support affected populations. For example, economic losses and damages from disasters in 1982-83, 1997-98, and 2017 amounted to 11.6, 6.2, and 1.6 percent of GDP, respectively (World Bank, 2016). Approximately 40 percent of total damages in 2017 were inflicted on the road network, claiming a portion of the county's fiscal space to fund reconstruction of pre-existing public infrastructure. Moreover, the IMF-adapted ND-GAIN index ranks Peru as the most vulnerable country in Latin America 5 (LA5) to chronic physical risks—the slow moving changes in temperature and precipitation norms.

This vulnerability underscores the importance of quantifying long-term output losses associated with physical climate risks and evaluating the potential returns on policies aimed at containing them. Given the multitude of competing policy priorities and often limited fiscal space, governments must carefully allocate resources across a wide range of needs (IMF, 2020). Quantitative assessments, such as the one presented in this paper, can inform cost-benefit analyses that should support policymakers' decision-making (Bellon and Massetti, 2022a). In Peru's case, any credible long-term assessment must be grounded in a clear understanding of the short-term macroeconomic impacts of its most frequent and disruptive weather-related shock—El Niño Costero.

To this end, this paper begins by estimating the impact of El Niño Costero events on Peru's economy between 1980 and 2023 using the Local Projection method (Jordà, 2005). We find that strong to very strong El Niño Costero events typically trigger temporary but severe inflationary pressures, sharp contractions in agricultural output and fish production, and a reduction in the fiscal space. On average, fish production falls by 70 percent and agricultural output by 11 percent in the year following a strong El Niño episode, with recovery to pre-shock trends typically taking over a year. These shocks also tend to be fiscally costly, as disaster-related expenditures increase while tax revenues fall due to reduced economic activity, reducing the primary balance by 2 percentage points of GDP. Additionally, we present evidence of an inflation pass-through from non-core to core prices that takes approximately one calendar year to materialize.

Building on these estimates, we project Peru's potential output through 2100 under three climate scenarios—SSP1-2.6, SSP2-4.5, and SSP3-7.0—by distinguishing between chronic and acute physical risks. Acute risks are modelled using an extended version of the regime-switching DSGE framework developed by Fernandez-Corugedo et al. (2023), extended to include non-destructive repeated disaster shocks in the spirit of drought shocks in Gallic and Vermandel (2020). Chronic risks are quantified under the assumption of gradual natural adaptation by the population, using output elasticity estimates from Chirinos (2021). Our simulations produce

larger output losses than those reported in earlier studies, with cumulative income losses estimated between 13.9 and 18.6 percent of GDP by 2050, rising to between 22.0 and 50.6 percent of GDP by 2100.

We then evaluate the real and fiscal benefits of strengthening the structural resilience of public infrastructure and closing implementation gaps in the country's national adaptation plan and disaster risk management strategy. These measures could yield significant economic dividends, with potential output projected to increase by 9.3 to 12.3 percent by 2050 and 12.4 to 31 percent by 2100 (relative to a baseline with extreme weather events and persistent temperature changes). However, these gains tend to materialize gradually and are backloaded, falling short of fully offsetting the losses expected from chronic and acute physical climate risks.

Importantly, our analysis also suggests that such expenditures can be fiscally self-sustaining over the long term. By reducing the need for post-disaster reconstruction and emergency relief, while expanding the tax base through stronger growth and resilience dividends, they generate positive net fiscal savings. These savings—measured as the difference between fiscal gains and the costs of measures—are estimated to range from 1.2 to 1.6 percent of GDP per annum by 2050, and from 2.3 to 4.6 percent of GDP per annum by 2100.

The structure of the paper is as follows. Section 1.1 reviews the related literature. Section 2 examines Peru's vulnerability to both acute and chronic physical risks. Section 3 presents an empirical analysis of the macroeconomic impact of El Niño Costero events on key macroeconomic indicators. The structural framework used to quantify output losses from physical risks is introduced in Section 4. Section 5 explores the potential benefits of investing in structural resilience and adaptation. Section 6 concludes.

### 1.1 Literature overview

There is a growing literature on the macroeconomic impacts of climate phenomena at the global level, particularly from El Niño events. Cashin et al. (2017) employ a GVAR model for 21 countries showing that the impacts of El Niño shocks on growth, inflation and commodity prices are highly heterogeneous, varying from growth declines in Australia and Chile to improvements in the US and Europe. Building on this work, Smith and Ubilava (2017) focus specifically on developing countries, finding El Niño events reduce GDP growth by 1-2 percent annually, with stronger effects in tropical regions. Our study extends these findings by providing detailed analysis of El Niño's sectoral impacts for a country that is highly vulnerable due to its geography, reliance on climate-exposed sectors, and lack of resilient infrastructure.

Regional studies have highlighted Peru's particular vulnerability to climate change. Chirinos (2021) studies the effect of longer-term, slower changes to climate, measured by anomalies from historical norm in precipitation and temperature in Peru, projecting a 9 percent reduction in per capita income by 2050 with agriculture and fisheries at greatest risk. SENAMHI (2009) uses global and regional models incorporating national climate trends to predict changes in

temperature and precipitation patterns by 2030, emphasizing the heterogeneous climate impacts across Peru's diverse geography. Our study takes as inputs potential climate scenarios for Peru and the estimated costs of longer-term climate changes, building on this literature by quantifying not only the costs of inaction, but also the potential benefits of adaptation, estimating that investments in climate resilience could yield substantial output gains and fiscal savings.

The methodological literature has evolved from early efforts like Choi and Fisher (2003), which employ a 3SLS regression framework to quantify the expected losses from increased natural disasters generated by human-induced climate change. Auffhammer (2018) highlights challenges in early studies quantifying climate damages, such as panel data techniques for studying effects which are heterogeneous across regions and time and the limitation of analysis focusing only on short-run (intensive margin) or long-run (extensive margin) adaptation to weather fluctuations. Recent papers have addressed these challenges through various modelling approaches. Gallic and Vermandel (2020) develop a DSGE model for studying weather shocks to agricultural productivity, which they calibrate with SVAR model estimates on the short-run effect of weather events in New Zealand. Fernandez-Corugedo et al. (2023) introduce a Markov-switching dynamic model for small open economies (hereafter, the FGG model) to study the long-run macroeconomic returns from adaptation investment to reduce long run-losses from extreme climate events like those faced by small states in the Caribbean and Pacific. We build on their work by adapting the FGG model to more frequent but less severe weather events, such as those triggered by El Niño.

## 2 Peru's vulnerability to climate shocks

The prevailing physical risk profile of Peru is dominated by floods, landslides, droughts, and storms (Figure 1, panel *a*). These shocks have followed historical patterns. Peru is particularly exposed to the El Niño Costero phenomenon, a recurring warming of the sea surface temperature along its coast (Niño 1+2 region) occurring every four to five years. El Niño years are marked by increased asset losses and a larger affected population due to intensification of natural disasters (Figure 1, panel *b*). Furthermore, the country's complex geography and hydrology result in a wide range of impacts that systematically vary across regions. In the northern coast, which typically lacks precipitation, heavy rainfall translates into substantial infrastructure damages from floods, lower agricultural yields, and a slowdown in the construction sector. In the southern regions, El Niño Costero manifests as a reduction in precipitation that reduces rain-fed agriculture's output. Moreover, the rise in the sea surface temperature during El Niño Costero adversely affects fish production along Peru's coastline (e.g., lower anchovy catches) and associated manufacturing activities (e.g., processing of fishmeal and fish oil), while higher air temperatures across the country disrupt flowering and pollination (e.g., blueberries, avocados, mangoes, olives). All of the above results in an uneven distribution of physical risks across time, geography, and economic sectors, which put a drag on economic growth.

Beyond the immediate impacts associated with the current disaster profile, climate change is projected to significantly reduce the productivity of key economic sectors, particularly agriculture and fisheries. Peru is the most vulnerable country to climate change among the Latin America 5 (LA5) group and the third most vulnerable country in Latin America (IMF-adapted

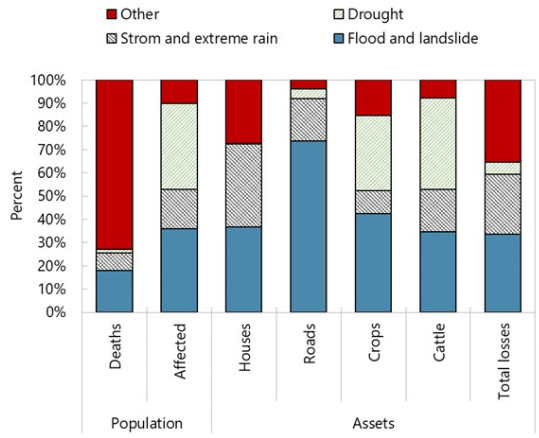


(a) Share of population affected and asset losses by type of disaster.

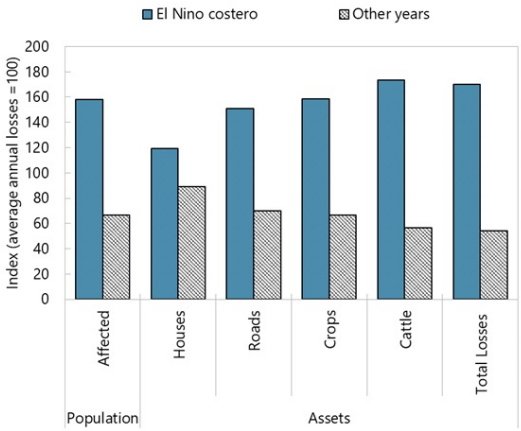


(b) The index of economic losses and El Niño Costero.

Figure 1: Peru's disaster loss profile.

Source: IMF staff calculation using United Nations DesInventar database.

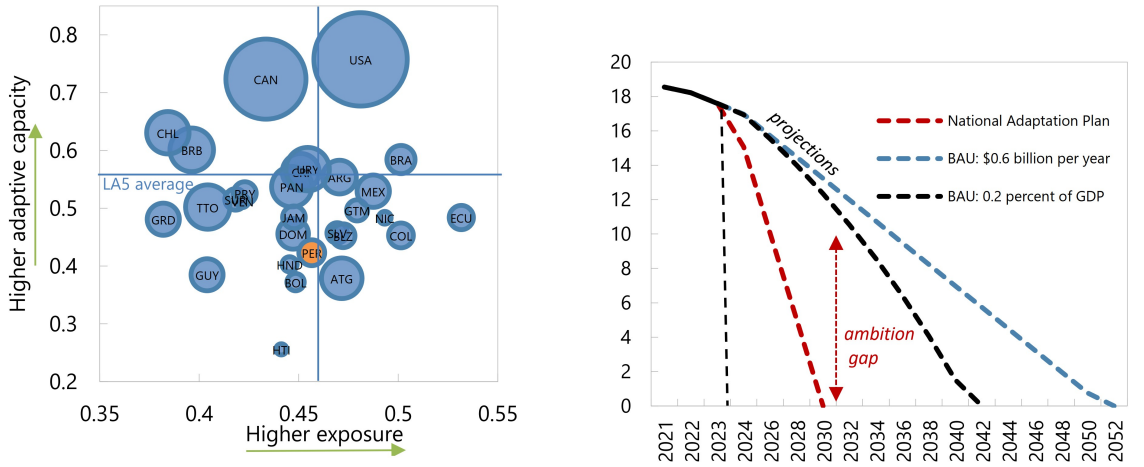


(a) Adaptive capacity and exposure to climate change in the Americas.

(b) Projection of Peru's remaining adaptation needs (USD, billions).

Figure 2: Adaptive capacity and investment needs.

Source: IMF-adapted ND-GAIN index, IMF staff calculation using authorities' data.

ND-GAIN, 2021). Climate change is expected to undermine the country's natural capital and exacerbate water shortages, likely reducing the stock of fish in the Humboldt current (Salvatteci et al., 2022) and lowering crop yields across the board (World Bank, 2022). Peru's economy is dependent on these resources as agriculture and fish production jointly constitute 7.6 percent of GDP and employ 28 percent of the workforce (OECD, 2023). Moreover, these sectors represent a notable part of the country's trade with the rest of the world, accounting for over 18 percent of total exports. Medium-term climate variability is also expected to intensify under climate change scenarios. Cai et al. (2021) suggest that El Niño-related precipitation patterns in the equatorial Pacific will become more intense and shift eastward.

Importantly, Peru's vulnerability to climate change predominantly reflects one of the lowest adaptive capacities in the region (Figure 2, panel *a*). The wide gap in adaptive capacity relative to LA5 peers, can be attributed to insufficient water management capacity (e.g., dams, water treatment plants), as well as a relatively low quality of infrastructure (e.g., ports, railroads, roads, information technology). Moreover, the potential to enhance adaptive capacity is hindered by weak public investment management, poor coordination across different levels of government, and capacity constraints within the civil service. Combined with the chronic under-execution of capital budgets, these factors pose significant barriers to effective investment in structural climate resilience. If the recent pace of implementation of measures outlined in the National Adaptation Plan persists, the country is likely to miss national targets for strengthening its structural resilience and continue experiencing devastating impacts from climate shocks (Figure 2, panel *b*).

# 3 Empirical evidence

El Niño events in Peru are often associated with significant damages to private and public capital stocks, which are documented through data on economic losses in major disaster databases (e.g., EM-DAT and DesInventar). However, these events also tend to influence the stock of natural capital and productivity of some economic activities (e.g., agriculture, fisheries, construction) through channels that are more difficult to account for.

This section aims to quantify the overall economic impact of El Niño Costero on Peru by estimating impulse response functions for sectoral output, prices, and key fiscal indicators. It begins by outlining the data sources and empirical methodology, followed by a presentation and discussion of the main results.

## 3.1 The model

We use the local projection method proposed by Jordà (2005) to estimate impulse response functions for strong El Niño events. The impact of an average strong El Niño Costero shock is estimated for a 1–2 year horizon using the equation below:

$$y_{t+h} - y_{t-1} = \beta_0^h + \beta_1^h shock_t + \sum_{j=1}^{4} \theta_j^h \Delta y_{t-j} + \sum_{i=1}^{M} \alpha_i^h x_{t-1}^i + \nu_t^h \tag{3.1}$$

where $y_{t+h} - y_{t-1}$ represents the cumulative percent change in the dependent variable from period $t-1$ to $t+h$, $shock_t$ captures the El Niño Costero shock, while $\Delta y_{t-j}$ denotes the $j$-th lag of the dependent variable's growth rate. The term $x_{t-1}^i$ refers to the logarithm of the $i$-th control variable from a set of $M$ controls. For each horizon $h$ of the impulse response function (IRF), $\beta_0^h$ is the intercept, $\beta_1^h$ measures the response of the dependent variable to the shock, and $\theta_j^h$ and $\alpha_i^h$ are the coefficients associated with the lags of the dependent variable and the control variables, respectively.

## 3.2 Identification of the El Niño shock and data

El Niño refers to the warm phase of the El Niño–Southern Oscillation (ENSO), a periodic fluctuation in sea surface temperatures across the central and eastern Pacific Ocean. Its counterpart, La Niña, represents the cool phase of the cycle. In the Peruvian context, El Niño events are typically classified into two types: Costero and Global. This distinction is based on the location of the temperature anomalies in the Pacific Ocean. El Niño Costero events originate in the Niño 1+2 region, near the coast of Peru, whereas El Niño Global events are associated with anomalies in the Niño 3.4 region.

To apply the Local Projection method for assessing the impact of El Niño events on Peru's economy, we first define and construct El Niño shocks. We use sea surface temperature (SST)

anomaly data for the Niño 1+2 region, obtained from the National Oceanic and Atmospheric Administration (NOAA), as all historical El Niño Costero episodes are characterized by pronounced and persistent SST increases in this region (Figure 3). To isolate persistent SST increases from white noise, we compute a 3-month rolling average of the SST anomaly, yielding a variant of the Oceanic Niño Index (ONI). An El Niño Costero episode is defined as beginning in the month when this index exceeds +0.5°C. Shocks are then defined as binary variables equal to 1 in the first month or quarter of each identified event (depending on the estimation frequency) and 0 otherwise. This analysis focuses on strong and very strong events, restricting the sample to episodes in which the index exceeds +1.5°C at any point during an identified event. This procedure yields five shocks in our quarterly sample and four shocks in our monthly sample between.

We estimate IRFs for core and headline inflation at monthly frequency and for sectoral output and the primary fiscal balance at quarterly frequency. All variables are either seasonally adjusted by Haver or using E-views X-13. We construct inflation by taking CPI data from Banco Central de Reserva del Perú (BCRP) and calculating the year over year growth rate. We obtain data on sectoral output and the central government's primary balance from Haver Analytics and BCRP. Our monthly sample covers the period from January 1992 to September 2023, while our quarterly sample spans from the first quarter of 1990 to the third quarter of 2023.

The set of $M$ controls includes (a) oil price indices for Peru's main oil import partners, (b) a global fertilizer index, and (c) a local production index for monthly frequency estimates. The set of controls for the quarterly estimates excludes the local production index.

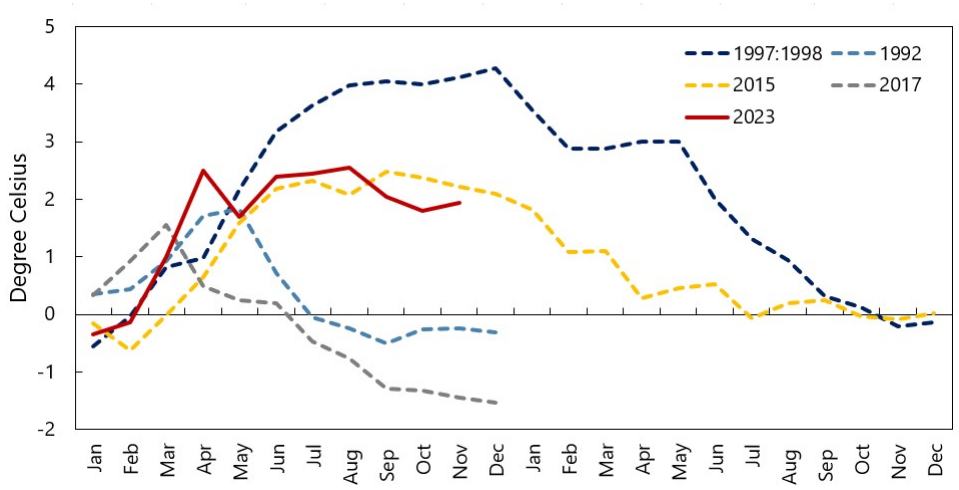


Figure 3: Sea surface temperature anomaly in the Niño 1+2 region during past El Niño Costero events.

Source: National Oceanic and Atmospheric Administration.

### 3.3 Short-term macro-fiscal implications of El Niño shocks

Our results indicate that strong El Niño events have historically been associated with inflationary pressures in Peru. Specifically, strong El Niño Costero episodes tend to increase both headline and core inflation. The impact on headline inflation is immediate, peaking at a 4.4 percentage point year-over-year increase by the end of the first year before gradually declining and turning negative as prices revert toward pre-El Niño levels. In contrast, the effect on core inflation is more gradual, with a noticeable increase emerging about 12 months after the initial shock—suggesting a potential pass-through from headline to core inflation (Figure 4, panel *a*).

One of the main channels through which El Niño affects inflation is via food prices. The increase in non-core food inflation—which captures price fluctuations in perishable items such as fresh fruits and vegetables—closely follows the trajectory of headline inflation but with significantly greater magnitude (Figure 4, panel *b*). Non-core food inflation peaks at an 8.1 percentage point increase by the end of the first year. In contrast, core food prices, which are less sensitive to weather shocks, begin to rise in the second year, reaching a 2.3 percentage point increase in the inflation rate about 20 months after the onset of an El Niño Costero event. Consistent with these historical patterns, the 2023 El Niño Costero triggered temporary spikes in year-over-year CPI inflation for the Fish and Seafood category—rising by 11 percentage points between February and June—and for Fruits, which saw a 22.6 percentage point increase between February and September.

Strong El Niño events typically last slightly longer than one year. Figure 5 presents the impulse response results for sectoral output, the primary fiscal balance, and the El Niño Costero

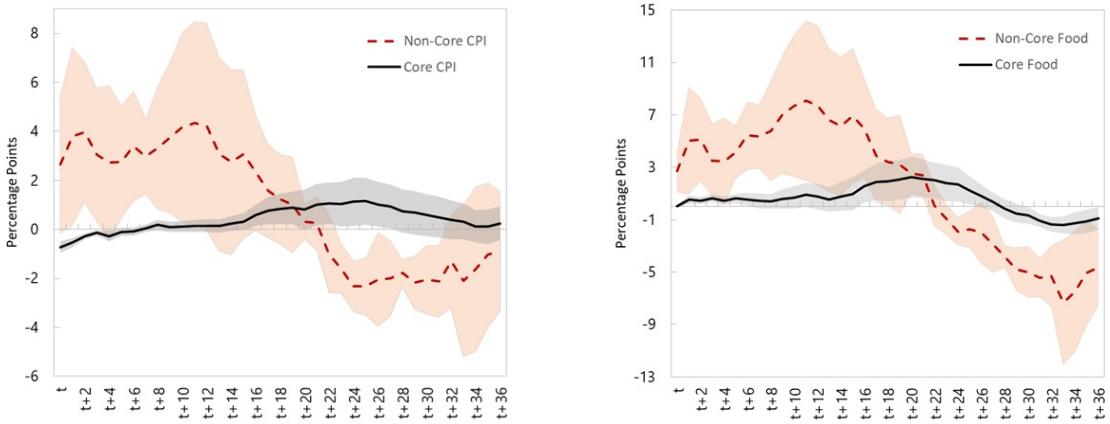


(a) Overall inflation rate.

(b) Food inflation rate.

Figure 4: Year-over-year monthly inflation increase following a strong El Niño Costero.

Source: Source: IMF staff calculation.
Note: Shaded areas present the 68 percent confidence interval.

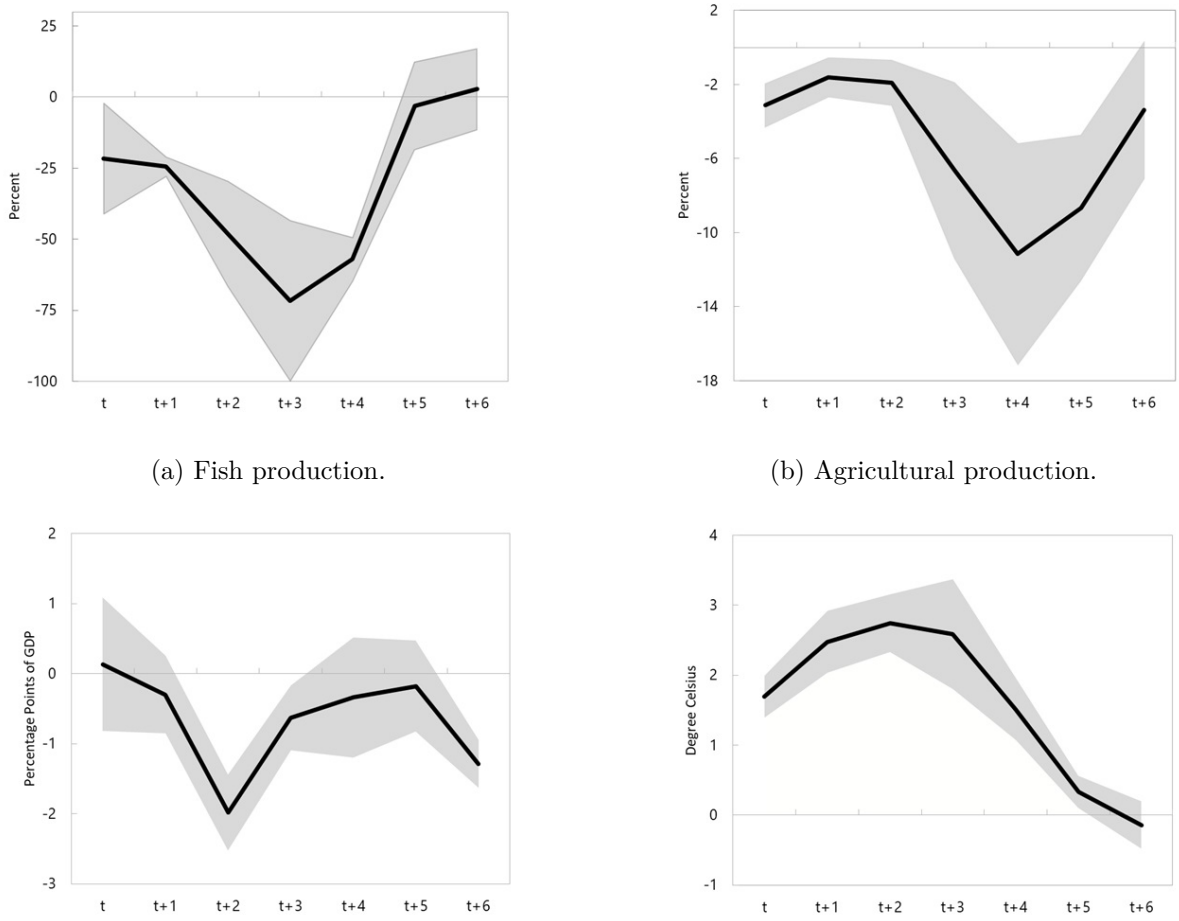


(a) Fish production.

(b) Agricultural production.

(c) Primary balance.

(d) El Niño Costero index.

Figure 5: Change in sectoral output, primary balance, and the ONI index following a strong El Niño Costero shock.

Source: IMF staff calculations.
Note: Relative to a no-El Niño baseline. Shaded areas indicate the 68 percent confidence interval. "t+$x$" corresponds to $x$ quarters after the onset of the El Niño Costero event.

index. Within four quarters a strong El Niño Costero shock sharply reduces fishery and agricultural output. On average, fish production drops by 70 percent within the first year, followed by a rapid recovery as sea surface temperatures normalizes and fish stocks in the Humboldt Current are replenished. In contrast, agricultural output declines by about 11 percent over the same period but recovers more gradually. The impact on agriculture is more persistent, with output remaining 3.4 percent below pre-El Niño levels 18 months after the shock.

Accounting for spillover effects on the manufacturing sector, as well as the impact on construction and mining, El Niño Costero events typically reduce real GDP by approximately 5

percent within the first year. Increased public spending on infrastructure reconstruction and support for affected populations aims to contain the overall decline in output. The central government's primary balance generally deteriorates by about 2 p.p. of GDP within a year of the shock, reflecting both higher expenditures and reduced revenue collection.

These findings are consistent with the 2023 El Niño Costero episode in Peru, which reached the "strong" classification in April 2023. The event disrupted two fishing seasons and lowered agricultural yields. Between March and November 2023, fishing and agricultural output were 27.3 percent and 4.9 percent below trend, respectively, while construction and manufacturing output declined by 9.2 percent and 6.6 percent. Over the same period, the central government's annual primary balance to GDP ratio declined by approximately 1.2 p.p.

# 4 Long-term output losses from El Niño and climate change

As demonstrated in the previous section, recurring natural hazards already impose a significant burden on Peru's economy. As the country experiences repeated natural disasters, amplified by ENSO cycles, the cumulative impact of successive shocks results in persistent losses that weigh on long-term macroeconomic performance.[1] Combined with the likely intensification of existing climate shocks and the emergence of new, slower-moving climate change impacts, Peru is projected to follow a lower potential output trajectory in the future.

To quantify such trajectories, this section adopts a two-pronged approach. First, we use a Markov-switching general equilibrium model to estimate the impact of recurring and intensifying shocks on the long-run output level, capturing several key channels discussed earlier. Second, we combine temperature anomalies from Massetti and Tagklis (2023) and the growth-temperature elasticities from Chirinos (2021) to assess the effects of slow-moving climate change on growth—representing chronic climate risks. This approach provides a tractable way to decompose the overall challenge into two more manageable components. However, it rests on the simplifying assumption that acute and chronic climate risks are independent within our framework.

## 4.1 Modelling acute physical risk

The IMF's FGG model is used to quantify the long-term impact of natural disasters on the economy of Peru. The FGG model (Fernandez-Corugedo et al., 2023) is a Markov-switching dynamic small open economy DSGE model designed to evaluate the macroeconomic returns of investment in climate and disaster resilience. It assumes the economy alternates between two disaster regimes and includes two types of public capital: standard and resilient. Standard capital is vulnerable to disasters and partially destroyed in the disaster regime, while resilient capital is immune. Both are used in production alongside private capital and labor. This distinction is standard in the literature on the macroeconomic effects of natural disasters (Marto et al., 2018; Cantelmo et al., 2019).

The FGG model is extended to account for the impact of El Niño Costero on natural capital in determining macro-fiscal outcomes. Following the spirit of the approach in Gallic and Vermandel (2020), the baseline model is extended to include the natural capital in the production function:

$$\underbrace{Y_t}_{\text{Real GDP}} = \underbrace{\left[\theta(s)K^N\right]^{\omega}}_{\text{Available natural capital}} \left[ \underbrace{(K^G_{t-1})^{\alpha_G}}_{\text{Public capital}} \underbrace{z_t}_{\text{TFP}} \overbrace{(N_t)^{1-\alpha_k}(K_{t-1})^{\alpha_k}}^{\text{Private factors of production}} \right]^{1-\omega} \tag{4.1}$$

[1] Both positive and negative temperature anomalies, driven by ENSO cycles, have significant effects on economic activity. Both El Niño and La Niña have capacity to affect output in primary sectors, but this paper focuses exclusively on assessing the economic losses associated with El Niño events.

where $\theta(s)$ is the parameter capturing the impact of natural disasters on natural capital, $K^N$ is the stock of natural capital, $z_t$ is the total factor productivity productivity, $K^G_{t-1}$ is the stock of public capital, $N_t$ is the labor input, and $K_{t-1}$ is the stock of private capital. The elasticity of output with respect to natural capital is denoted by $\omega$, to public capital by $\alpha_G$, and to private capital by $\alpha_K$.

A key feature of the model is the use of a Markov-switching structure, which allows parameter values to shift across different regimes. These regime-dependent parameters are indexed by $\cdot(s)$, where $s$ represents the state of the economy. Our model includes two states: one where natural disasters cause moderate damage and another where the impact is significantly amplified due to the presence of El Niño Costero. In line with the standard FGG framework, natural disasters reduce the stock of physical capital; however, in our extension, they also temporarily degrade the country's stock of natural capital. Moreover, the total stock of public capital now includes adaptation capital, which mitigates the adverse effects of climate events on natural capital by influencing the parameter $\theta(s)$. These shifts between states are governed by the probabilities of transition, which we calibrate using quarterly data on El Niño occurrences between 1990 and 2023. The transition matrix $P_{s_t,s_{t+1}}$ is given by:

$$P_{s_t,s_{t+1}} = \begin{bmatrix} p_{1,1} & p_{1,2} \\ p_{2,1} & p_{2,2} \end{bmatrix} = \begin{bmatrix} 0.883 & 0.117 \\ 0.311 & 0.689 \end{bmatrix} \tag{4.2}$$

where $p_{1,1}$ denotes the probability that a non–El Niño quarter is followed by another non–El Niño quarter, while $p_{1,2}$ represents the probability that a non–El Niño quarter is followed by an El Niño quarter. Conversely, $p_{2,2}$ is the probability that an El Niño quarter is followed by another El Niño quarter, and $p_{2,1}$ is the probability that an El Niño quarter is followed by a non–El Niño quarter. The transition matrix implies an unconditional probability of 26.01 percent for observing an El Niño Costero quarter in our sample.

The impact of strong and very strong El Niño shocks on physical capital is calibrated at 2.6 percent of the capital stock per quarter, based on the average damages reported for select severe events in World Bank (2016, 2022). The impact on natural capital, $\theta(s)$, is set to ensure that the total output loss estimated in Section 3 is consistent with the output losses implied by physical capital damages. Weak and moderate El Niño shocks are assumed to cause one-fourth of the damages and output losses associated with strong and very strong events. The impact of other natural disasters (unrelated to El Niño) is calibrated by dividing the average El Niño impact by 3.13, based on the differential in total losses between El Niño Costero years and other years as recorded in the DesInventar database (Figure 1, panel *b*).

Table 1: Key Parameters for the Steady State

| Parameter | Description | Value |
|---|---|---|
| $\omega$ | Output elasticity to natural capital | 0.2 |
| $\eta$ | Scale factor in the utility function | 4.3 |
| $\xi$ | Inverse Frisch elasticity | 0.5 |
| $\beta$ | Discount factor | 0.99 |
| $\epsilon_w$ | Elasticity of substitution between labor varieties | 6 |
| $\alpha_g$ | Share of public capital on the production function | 0.1 |
| $\alpha_K$ | Share of private capital on the production function | 0.2 |
| $\delta_{gr}$ | Depreciation rate of public resilient capital | 0.06 |
| $\alpha_I$ | Share of imported goods for investment | 0.5 |
| $\alpha_C$ | Share of imported goods in the consumption basket | 0.3 |
| $\eta_I$ | Elasticity of import substitution for investment goods | 0.75 |
| $\eta_C$ | Elasticity of import substitution for consumption goods | 0.75 |
| $\eta_X$ | Elasticity of exports to the exchange rate | 0.5 |
| $a^{Gr}$ | Price mark-up for resilient investment goods | 1.25 |
| $\phi_b$ | Fiscal reaction function parameter | 0.1 |
| $\varepsilon$ | Public investment efficiency | 0.48 |
| $B/Y$ | Net Government Debt over GDP | 0.23 |
| $G_C/Y$ | Government consumption over GDP | 0.114 |
| $G_I/Y$ | Government investment over GDP | 0.052 |
| $\tau/Y$ | Tax revenues over GDP | 0.42 |
| $Rem/Y$ | Remittances over GDP | 0.015 |
| $\bar{R}_t^*$ | External interest rate (annual) | 0.05 |
| | **Regime Switching Parameters** (1 = No El Niño Costero, 2 = El Niño Costero) | |
| $g^A(1)$ | Growth rate | 0.028 |
| $g^A(2)$ | | 0.011 |
| $\delta_Y(1)$ | Depreciation rate private capital | 0.06 |
| $\delta_Y(2)$ | | 0.07 |
| $\delta_{gnr}(1)$ | Depreciation rate public non-resilient capital | 0.07 |
| $\delta_{gnr}(2)$ | | 0.11 |
| $\theta(1)$ | Utilization of natural capital | 0.993 |
| $\theta(2)$ | | 0.978 |

Moreover, Cai et al. (2021) project that ENSO-related rainfall in the equatorial Pacific

will intensify and shift eastward under severe climate change, leading to a 59 percent increase in the frequency of strong El Niño events by the second half of the century. To reflect this expected intensification, we increase the anticipated losses from an average El Niño Costero event accordingly. For further details on the model, see Fernandez-Corugedo et al. (2023). Key parameters used to calibrate the model and compute the steady state are presented in Table 1

In our application, the FGG model is a tool used to produce the long-run (steady-state) level of potential output under various assumptions about disaster impacts. This output level is then combined with an estimate of losses from chronic climate risks to produce potential GDP trajectories, as described in the next section. The model equations are presented in Appendix A, while a full discussion of modelling assumptions are detailed in Fernandez-Corugedo et al. (2023).

### 4.2 Modelling chronic physical risk

Although there is no consensus on magnitudes, most studies agree that temperature increases tend to undermine economic growth (Tol, 2009; Burke et al., 2013; Kahn et al., 2021; Mohaddes and Raissi, 2024). Furthermore, adaptation is not a new phenomenon: individuals, firms, and societies have long adjusted to changing climatic conditions, enabling economic specialization and resilience (Seo and Mendelsohn, 2008; Kurukulasuriya et al., 2011; Di Falco and Veronesi, 2013; Kahn, 2016; Bellon and Massetti, 2022a). It follows that a realistic framework should account for temporary declines in economic growth while also allowing for agents to gradually adapt to slow-moving shifts in climate norms.

To capture the uncertainty surrounding future changes in temperature norms, we produce three distinct projections of potential output through 2100, each corresponding to a different global warming scenario. The first is an aspirational scenario aligned with the Paris Agreement, SSP1-2.6 (Paris). The second, SSP2-4.5 (Intermediate), reflects a continuation of historical warming trends, and is broadly consistent with current policies. The third is a pessimistic scenario, SSP3-7.0 (Hot), which assumes policy reversals and higher emissions.

For each scenario $i$, we decompose potential output trajectories into a time invariant steady state level and a time varying component:

$$\underbrace{\tilde{Y}_t}_{\text{Potential GDP}} = 4 \times \underbrace{\bar{Y}}_{\text{Quarterly SS GDP}} \times \underbrace{T_t^i}_{\text{Time-varying trend}} \tag{4.3}$$

where $\tilde{Y}_t^i$ is the real value of the country's potential output at time $t$, $\bar{Y}$ is the quarterly steady state potential output level, and $T_t^i$ is a time-varying component that is influenced by tempera-

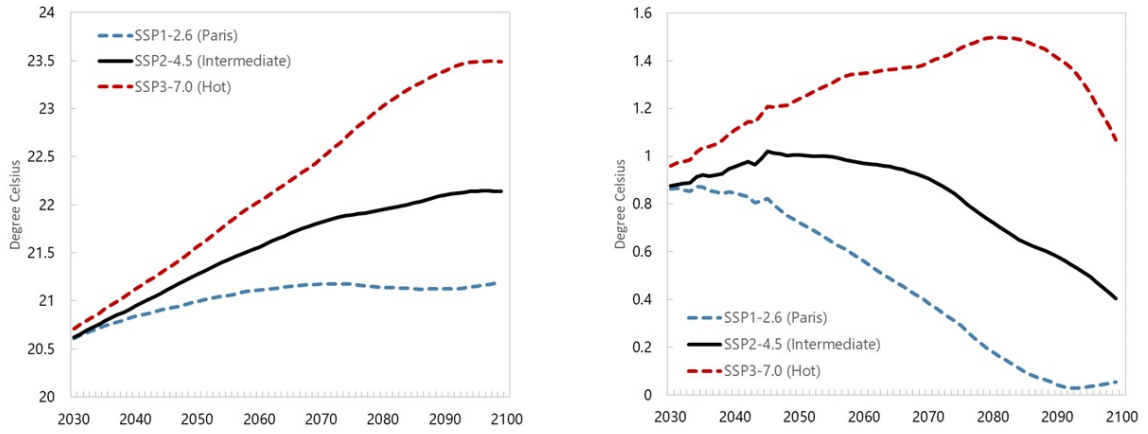


(a) Average annual temperature.

(b) Temperature anomaly relative to a rolling 30-year temperature norm.

Figure 6: Temperature projections under climate change scenarios.

Source: IMF staff calculation using Massetti and Tagklis (2023).

ture anomalies:

$$\underbrace{\frac{T_t^i}{T_{t-1}^i}}_{\text{Trend growth}} = 1 + \underbrace{g^{SS,i}}_{\text{Net SS growth}} - \overbrace{\alpha\left[\underbrace{t_t^i}_{\text{Avg. annual temp.}} - \underbrace{\frac{1}{N}\sum_{m=1}^{N} t_{t-P-m}^i}_{\text{Rolling temp. norm}}\right]}^{\text{Temp. anomaly}} \tag{4.4}$$

where $g^{SS,i}$ is the stationary steady state potential output level, $t_t^i$ is the average annual temperature rate recorded in Peru in year $t$, and $\frac{1}{N}\sum_{m=1}^{N} t_{t-P-m}^i$ is the temperature norm calculated as a rolling $N$-year temperature average (i.e., between years $t-P-N$ and $t-P$). $\alpha$ is the elasticity governing the reduction in the net annual growth rate to increases in temperature anomaly.

We calculate temperature anomalies for Peru using temperature data from Massetti and Tagklis (2023). Figure 6, panel *a* presents the average annual temperature, while Figure 6, panel *b* shows the resulting temperature anomalies, derived using $N = 30$ and $P = 15$. The steady-state growth rate, $g^{SS,i}$, is aligned with the FGG model assumptions. To construct output trajectories, we combine steady-state growth with a time-varying trend. The time-varying trend is derived by linking temperature anomalies to output losses, using separate elasticities for changes in maximum and minimum temperatures, and then averaging the effects on the trend. Specifically, the elasticity of output losses to minimum temperature changes is 0.4, while the elasticity for maximum temperature changes is 1.0, both taken from Chirinos (2021).[2]

[2]Country-specific output elasticities to average temperature changes are not available for Peru; hence, we rely on average effect between minimum and maximum temperature changes.

### 4.3 Output losses under climate change scenarios

The resulting potential output losses increase over time but depend on the assumed progress with the global mitigation effort. Combining the additional impact of climate change with the existing losses from climate, potential output could be up to 13.9-18.6 percent lower by 2050 and 22.0-50.6 percent lower by 2100, relative to the no climate change counterfactual (Figure 8, panel *a*). This is equivalent to a 0.1-0.3 percentage point reduction in the average annual potential growth rate due to climate and climate change (Figure 8, panel *b*).

Importantly, our estimated losses exceed those reported for Peru in Mohaddes and Raissi (2024) and Kahn et al. (2021). Using the same definitions for climate change scenarios, Mohaddes and Raissi (2024) projects economic losses for Peru of 0.7–10 percent by 2050 and 1–25 percent by 2100, relative to a no–climate change baseline. However, unlike our approach, these estimates are based on cross-country averages of gradual climate change impacts and do not incorporate the effects of increased disaster intensity.

In all scenarios except SSP3-7.0, potential growth losses are front-loaded. This pattern reflects the projected deceleration of global warming under SSP1-2.6 and SSP2-4.5, with temperature anomalies gradually returning to zero over the long term. For instance, under SSP1-2.6, the temperature anomaly converges to zero shortly before 2100, implying that the potential growth rate eventually aligns with the no–climate-change scenario. However, despite this convergence in growth rates, the level of GDP remains permanently lower due to losses experienced earlier. Beyond this point, the GDP trajectories under SSP1-2.6 and the no–climate-change scenarios evolve in parallel.

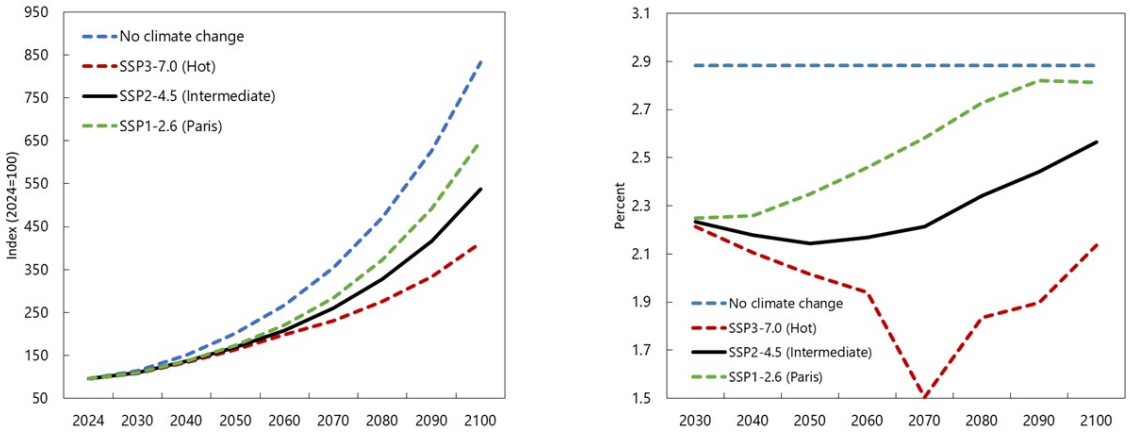


(a) Potential GDP level.

(b) Potential GDP growth rate.

Figure 7: Potential output under climate change scenarios.

Source: IMF staff calculation using the FGG model (Fernandez-Corugedo et al., 2023) and Massetti and Tagklis (2023).

Several limitations of our approach warrant consideration. First, the construction of temperature anomalies relies on median climate model projections, omitting model uncertainty. Second, the elasticities from Chirinos (2021) are backward-looking, and applying them to future scenarios assumes no change in technological progress, adaptive capacity, or policy-driven market responses. Third, Cai et al. (2021) simulate rising El Niño Global intensity under RCP8.5, while we assume similar increases under the less severe SSP3-7.0 scenario—likely leading to an overestimation of climate change costs under SSP3-7.0.

# 5 Macro-fiscal implications of climate resilience

To mitigate future output losses from climate shocks, the authorities established a legal framework for climate change in 2018 and developed national strategies for climate adaptation and disaster risk management. Progress has been made in strengthening public infrastructure, enhancing financial resilience, and identifying key adaptation gaps. However, climate-related spending remains limited, budget planning does not fully account for the cost of critical adaptation measures, and territorial planning requires further improvement. Overall, there is considerable scope to scale up investment in adaptation and resilience—particularly given that the potential benefits are expected to outweigh the costs—and to complement these efforts with reforms aimed at improving the quality of public investment to maximize returns.

To illustrate the benefits of closing adaptation gaps efficiently, we simulate a comprehensive reform package comprising three key components. First, we assume full implementation of the adaptation investments outlined in Peru's National Adaptation Plan by 2030. Secondly, we assume full implementation of the expenditures in Peru's National Disaster Risk Management Strategy by 2030. Thirdly, we incorporate climate-proofing of 80 percent of the country's public infrastructure. An estimate of the macro-fiscal benefits of this reform package is presented below.

## 5.1 Potential growth dividends

Our results indicate that investments in adaptation and structural resilience combined with increased public investment efficiency deliver sizable output gains in the long-term. Investing in resilience and adaptation offsets the impact of natural hazards and climate change on productive factors and growth. Structural resilience involves making public infrastructure, like roads, bridges, and schools, climate-proof, effectively representing a shift from standard to resilient capital. Adaptation investments cover expenditures on knowledge systems, irrigation and water management, and diversification of crops and livestock, among other items.[3] These investments reduce the impact of natural disasters on natural capital and productive government infrastructure, as well as partially offset the reduction in the long run growth rate due to positive temperature anomalies.

Based on discussions with the authorities, full implementation of measures in the National Adaptation Plan could mitigate up to one-third of the short-term impact of El Niño Costero on the country's natural capital. In the longer term, under the intermediate emissions scenario (SSP2-4.5), these measures are also expected to reduce by approximately one-third the adverse effects on productivity in the agriculture and energy sectors, as well as on labor productivity.

[3] Adaptation investments include expenses on pest management, resistant genetic resources, agricultural risk transfer systems, crop and livestock diversification, cultivated pasture conservation, soil erosion management and control technologies, soil fertilization, water supply and sanitation, multipurpose water storage, supporting technified irrigation, drainage systems, adapting landing sites for artisanal fishing, strengthening early warning systems, aquaculture management, among others.

Combined with the benefits from more resilience government infrastructure, total potential output gains can be as high as 9.3-12.3 percent by 2050 and 12.4-31 percent by 2100 (Figure 8).

While the proposed policy package does not fully offset the projected decline in potential output due to climate impacts, it remains cost-effective under all three global warming scenarios. As Bellon and Massetti (2022b) emphasize, adaptation programs should only be implemented if they yield a positive net present value (NPV) for society. This condition is met in the case of the measures analyzed in this paper, as they simultaneously enhance private sector surplus—by raising the income trajectory—and strengthen the government's fiscal position through net savings. However, a key risk to this assessment lies in the low quality of public investment and constraints related to absorptive capacity. These limitations are not explored in depth here and are left for future research.

### 5.2 Fiscal savings

When evaluating the appropriateness of large-scale productive spending programs, it is common to compare their growth dividends with the associated fiscal costs to get a measure of the bang for the buck. It is important to consider second-order fiscal effects in such assessments. Investments in climate resilience and adaptation not only boost productivity but also reduce physical damages to public capital. In turn, this lowers the need for reconstruction spending and emergency support to affected populations (avoided expenditures), while supporting a more stable (revenue stabilization) and, on average, higher stream of tax revenues (growth-induced revenue gains). If the returns on such investments are sufficiently high—either due to the availability of cost-effective solutions or high marginal returns driven by low existing capital stocks—they can generate net fiscal savings over the long term, effectively paying for themselves. Intuitively, this is especially true for countries most vulnerable to climate shocks and where average tax revenues constitute a relatively large share of national income.

To assess the magnitude and sign of net fiscal savings in Peru, we begin by quantifying the fiscal costs. Drawing on estimates from Aligishiev et al. (2022), climate-proofing infrastructure in the current investment pipeline, retrofitting existing public assets, and implementing coastal protection against sea level rise are projected to require an additional 0.4 percent of GDP in public investment between 2024 and 2030. Further spending needs related to disaster risk management—including the development of early warning systems, acquisition of emergency response equipment, and implementation of other components of the national disaster risk management strategy—are estimated at 0.2 percent of GDP in additional annual expenditure. Lastly, full implementation of the costed measures outlined in the National Adaptation Plan is expected to amount to 0.8 percent of GDP per year over the same period. Additionally, once these investments are made, we assume ongoing fiscal spending equal to 6 percent of the acquired public capital stock annually to cover depreciation and preserve the asset base.

Our analysis shows that public investments in adaptation and resilience in Peru are associated

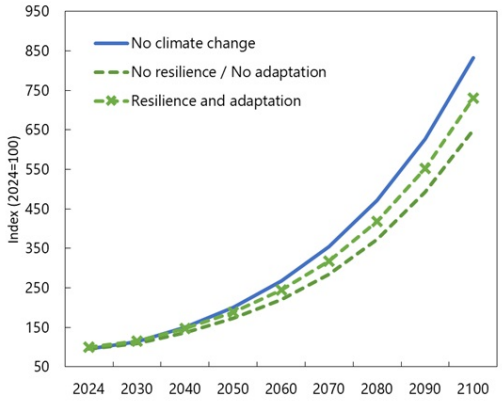


(a) SSP1-2.6 (Paris) scenario.

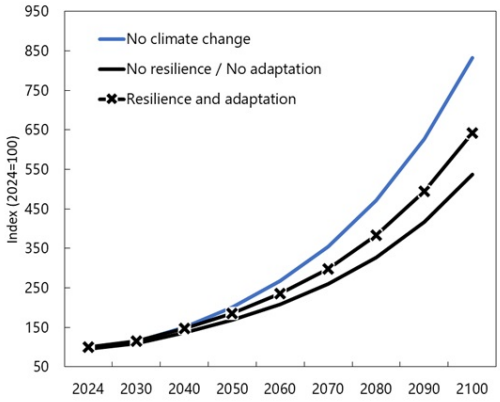


(b) SSP2-4.5 (Intermediate) scenario.

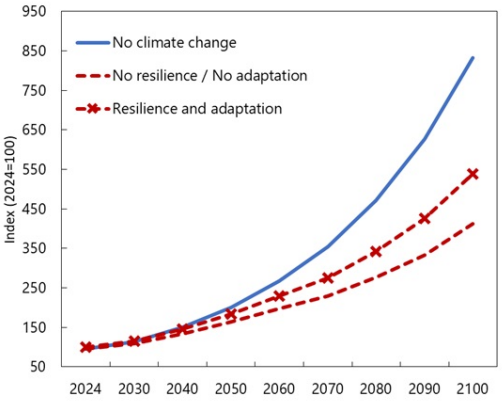


(c) SSP3-7.0 (Hot) scenario.

Figure 8: Potential GDP dividends from investments in resilience and adaptation across climate scenarios.

Source: IMF staff calculations based on the FGG model (Fernandez-Corugedo et al., 2023) and Massetti and Tagklis (2023).

with substantial long-term fiscal savings (Table 2). Between 2024 and 2050, these measures are estimated to generate average annual fiscal savings ranging from 1.2 to 1.6 percent of GDP (Figure 9, panel *a*). Over a longer horizon, from 2024 to 2100, average annual savings increase to between 2.3 and 4.6 percent of GDP. Notably, these savings are primarily driven by growth-induced revenue gains—that is, a higher GDP trajectory translates into a higher path for tax receipts. While the annual growth dividends are relatively modest and do not fully offset initial output losses, as discussed in Section 5.1, their cumulative effect over time leads to substantial increases in tax revenue levels by the end of the century.

Given that fiscal costs are incurred upfront while benefits accrue gradually over time, a

Table 2: Discounted Fiscal Savings from Investment in Resilience and Adaptation.
*(Present value at a 6 percent annual discount rate, in percent of 2023 GDP)*

| | SSP1-2.6 | | SSP2-4.5 | | SSP3-7.0 | |
|---|---|---|---|---|---|---|
| | 2050 | 2100 | 2050 | 2100 | 2050 | 2100 |
| **Total Return (a)** | 120.25 | 262.36 | 122.34 | 286.80 | 143.05 | 336.35 |
| Stock saving | 4.53 | 6.84 | 4.71 | 6.89 | 4.78 | 6.96 |
| Flow saving | 16.28 | 31.00 | 16.58 | 33.92 | 19.52 | 39.97 |
| Potential growth | 99.43 | 224.52 | 101.04 | 245.99 | 118.75 | 289.42 |
| **Total Cost (b)** | 10.53 | 11.65 | 10.53 | 11.65 | 10.53 | 11.65 |
| Adaptation | 4.84 | 4.92 | 4.84 | 4.92 | 4.84 | 4.92 |
| Resilience | 5.69 | 6.73 | 5.69 | 6.73 | 5.69 | 6.73 |
| **Net saving (a) - (b)** | 109.72 | 250.71 | 111.81 | 275.15 | 132.52 | 324.70 |

Source: IMF staff calculations using the FGG model (Fernandez-Corugedo et al., 2023), Massetti and Tagklis (2023), Harris et al. (2020), and Chirinos (2021).

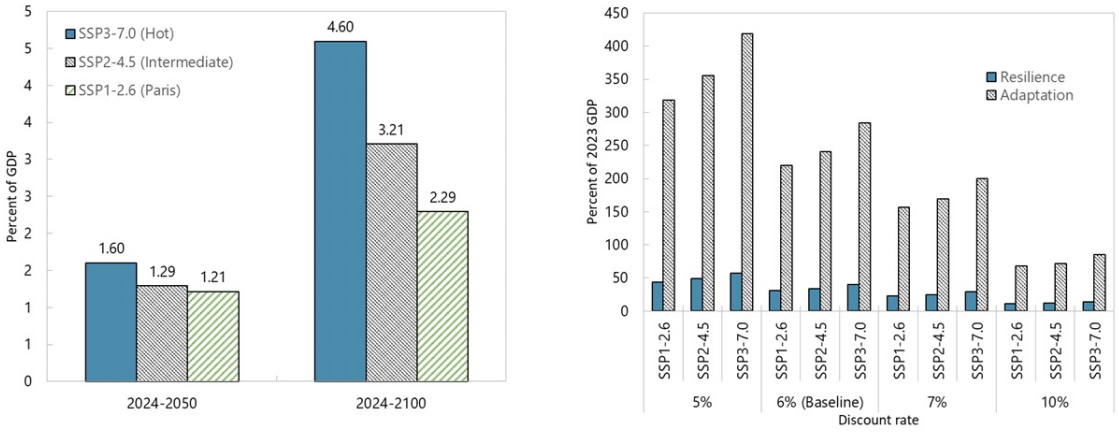


(a) Average annual fiscal savings.

(b) Present value of fiscal savings by 2100 under alternative discount rates.

Figure 9: Fiscal savings from investments in resilience.

Source: IMF staff calculation using the FGG model (Fernandez-Corugedo et al., 2023) and Massetti and Tagklis (2023).

proper assessment of cost-effectiveness requires evaluating fiscal savings in present value terms. This approach helps determine whether future benefits—realized decades later—are sufficient to justify the near-term investment. As shown in Figure 9, panel *b*, even after accounting for the time value of money and considering a range of discount rates, investments in adaptation and structural resilience remain cost-effective across all three global warming scenarios.

# 6 Conclusion

This study estimates the impact of El Niño Costero events on prices and economic activity in Peru, revealing significant inflationary effects and contractions in output of primary sectors. These empirical estimates are then used to calibrate a structural model, which, when combined with projections of chronic physical risks, yield substantial expected output losses by the end of the century. The analysis also shows that these losses can be partially offset through investments in structural resilience and climate adaptation—provided the quality of public investment improves. Importantly, such investments not only lift long-term output trajectories but could also be fiscally self-sustaining, as large fiscal savings materialize through reduced reconstruction needs and broader tax bases in the long term.

## References


Aligishiev, Z., Massetti, E., and Bellon, M. (2022). Macro-fiscal implications of adaptation to climate change. *IMF Staff Climate Note No 2022/002*.

Auffhammer, M. (2018). Quantifying economic damages from climate change. *Journal of Economic Perspectives*, 32(4):33–52.

Bellon, M. and Massetti, E. (2022a). Economic principles for integrating adaptation to climate change into fiscal policy. *IMF Staff Climate Note No 2022/001*.

Bellon, M. and Massetti, E. (2022b). Planning and mainstreaming adaptation to climate change in fiscal policy. *IMF Staff Climate Note No 2022/003*.

Burke, M., Hsiang, S., and Miguel, E. (2013). Global non-linear effect of temperature on economic production. *Nature*, (527):235–239.

Cai, W., Santoso, A., and Collins, M. (2021). Changing el niño–southern oscillation in a warming climate. *Nature Reviews Earth & Environment*, 2:628–644.

Cantelmo, A., Melina, G., and Papageorgiou, C. (2019). Macroeconomic outcomes in disaster-prone countries. *IMF Working Paper*, 19(217).

Cashin, P., Mohaddes, K., and Raissi, M. (2017). Fair weather or foul? the macroeconomic effects of el niño. *Journal of International Economics*, 106:37–54.

Chirinos, R. (2021). Efectos económicos del cambio climático en el perú. *Banco Central de Reserva del Perú Working Paper*, (2021-009).

Choi, O. and Fisher, A. (2003). The impacts of socioeconomic development and climate change on severe weather catastrophe losses: Mid-atlantic region (mar) and the u.s. *Climatic Change*, 58(1):149–170.

Di Falco, S. and Veronesi, M. (2013). How can african agriculture adapt to climate change? a counterfactual analysis from ethiopia. *Land Economics*, 89(4):743–766.

Fernandez-Corugedo, E., Gonzalez-Gomez, A., and Guerson, A. (2023). The macroeconomic returns of investment in resilience to natural disasters under climate change: A dsge approach. *IMF Working Paper*, 23(138).

Gallic, E. and Vermandel, G. (2020). Weather shocks. *European Economic Review*, 124.

Harris, I., Osborn, T., Jones, P., and Lister, D. (2020). Version 4 of the cru ts monthly high-resolution gridded multivariate climate dataset. *Scientific Data*, 7:1–18.

IMF (2020). Adapting to climate change in sub-saharan africa. *In Regional Economic Outlook: Sub-Saharan Africa—COVID-19: An Unprecendented Threat to Development*.

Jordà, (2005). Estimation and inference of impulse responses by local projections. *American Economic Review*, 95(1):161–182.

Kahn, M. E. (2016). The climate change adaptation literature. *Review of Environmental Economics and Policy*, 10(1):166–178.

Kahn, M. E., Mohaddes, K., Ng, R. N., Pesaran, M. H., Raissi, M., and Yang, J.-C. (2021). Long-term macroeconomic effects of climate change: A cross-country analysis. *Energy Economics*, 104:105624.

Kurukulasuriya, P., Kala, N., and Mendelsohn, R. (2011). Adaptation and climate change impacts: A structural ricardian model of irrigation and farm income in africa. *Climate Change Economics*, 02(02):149–174.

Maih, J. (2015). Efficient perturbation methods for solving regime-switching dsge models. *Norges Bank Working Paper*.

Marto, R., Papageorgiou, C., and Klyuev, V. (2018). Building resilience to natural disasters: An application to small developing states. *Journal of Development Economics*, 135:574–586.

Massetti, E. and Tagklis, F. (2023). Fadcp climate dataset: Temperature and precipitation. *Fiscal Affairs Department, International Monetary Fund*.

Mohaddes, K. and Raissi, M. (2024). Rising temperatures, melting incomes: Country-specific macroeconomic effects of climate scenarios. *Centre for Applied Macroeconomic Analysis Working Paper 42/2024*.

OECD (2023). Economic surveys: Peru 2023.

Salvatteci, R., Schneider, R., and Galbraith, E. (2022). Smaller fish species in a warm and oxygen-poor humboldt current system. *Science*, 375(6576):101–104.

SENAMHI (2009). Climate scenarios for peru till 2030. Technical report, National Service of Meteorology and Hydrology of Peru.

Seo, S. N. and Mendelsohn, R. (2008). An analysis of crop choice: Adapting to climate change in south american farms. *Ecological Economics*, 67(1):109–116.

Smith, S. C. and Ubilava, D. (2017). The el niño southern oscillation and economic growth in the developing world. *Global Environmental Change*, 45:151–164.

Tol, R. S. J. (2009). The economic effects of climate change. *Journal of Economic Perspectives*, 23(2):29–51.

World Bank (2016). Peru: A comprehensive strategy for financial protection against natural disasters.

World Bank (2022). Peru country climate and development report. CCDR Series, Washington, DC.

# Appendices

## A The FGG model

The model of Fernandez-Corugedo et al. (2023) is a Markov-switching dynamic stochastic general equilibrium (DSGE) framework designed to evaluate the macroeconomic impact of recurrent climate-related natural disasters and the returns to public investment in resilient infrastructure. The model incorporates critical features such as financial frictions with collateral constraints, heterogeneous households, endogenous risk premia, foreign remittances, and a comprehensive fiscal sector.

We simulate the stationarized version of the modified model using a first-order perturbation implemented in the RISE toolkit (Maih, 2015). The full set of first-order conditions used to inform results in Sections 4 and 5 is presented below, maintaining the original notation from Fernandez-Corugedo et al. (2023). For further details, including variable definitions and explanations, readers are referred to Fernandez-Corugedo et al. (2023) and Section 4 of this paper.

$$\tilde{\Delta}_t^K = \frac{1}{\tilde{C}_t^K(1+\tau^C)}$$

$$\tilde{\Delta}_t^K = \beta \left(\frac{1}{g_{t+1}^A}\right)^{\frac{1}{1-\alpha_K-\alpha_g}} \tilde{\Delta}_{t+1}^K \frac{z_{t+1}}{z_t} R_t^*$$

$$\tilde{\Delta}_t^K = \beta \left(\frac{1}{g_{t+1}^A}\right)^{\frac{1}{1-\alpha_K-\alpha_g}} \tilde{\Delta}_{t+1}^K R_t$$

$$\tilde{\Delta}_t^W = \frac{1}{(1+\tau^C)\tilde{C}_t^W}$$

$$(1+\tau_t^C)\omega \tilde{c}_t^W = (1-\tau_t^l)\tilde{W}_t \omega N_t + \tilde{T}_t^{GW}$$

$$\frac{1}{\eta}\left((1-\omega)\frac{\tilde{\Delta}_t^K}{(N_t^d)^\xi} + \omega \frac{\tilde{\Delta}_t^W}{(N_t^d)^\xi}\right)\tilde{W}_t(1-\tau_t^l) = \frac{\epsilon_W}{1-\epsilon_W}$$

$$\tilde{C}_t = \left[(1-a)^{\frac{1}{\eta}}(\tilde{C}_{H,t})^{\frac{\eta-1}{\eta}} + a^{\frac{1}{\eta}}(\tilde{C}_{F,t})^{\frac{\eta-1}{\eta}}\right]^{\frac{\eta}{\eta-1}}$$

$$\tilde{C}_{H,t} = (1-a)(p_{H,t})^{-\eta}\tilde{C}_t$$

$$\tilde{C}_{F,t} = a(z_t)^{-\eta}\tilde{C}_t$$

$$\tilde{C}_t = (1-\omega)\tilde{C}_t^K + \omega\tilde{C}_t^W$$

$$\tilde{I}_{H,t} = (1-a_I)\left(\frac{p_{H,t}}{p_t^I}\right)^{-\eta}\tilde{I}_t$$

$$\tilde{I}_{F,t} = a_I\left(\frac{z_t}{p_t^I}\right)^{-\eta}\tilde{I}_t$$

$$\tilde{I}_t = \left[(1-a_I)^{\frac{1}{\eta_I}}(\tilde{I}_{H,t})^{\frac{\eta_I-1}{\eta_I}} + a_I^{\frac{1}{\eta_I}}(\tilde{I}_{F,t})^{\frac{\eta_I-1}{\eta_I}}\right]^{\frac{\eta_I}{\eta_I-1}}$$

$$\tilde{I}_t = \tilde{I}_t^g + \tilde{I}_t^K + \tilde{I}_t^{G^n}$$

$$p_t^{gr} = \frac{p_t^I}{a^{gr}}$$

$$\tilde{Y}_t^H = (\theta(s)K_N)^{\omega}\left((g_t^A)^{\frac{\alpha_K+\alpha_g}{1-\alpha_K-\alpha_g}} z_t^Y \theta(s)(\tilde{K}_{t-1}^G)^{\alpha_g}(\tilde{K}_{t-1}^Y)^{\alpha_K}(N_t^d)^{1-\alpha_K}\right)^{1-\omega}$$

$$\tilde{Y}_t^H = \tilde{C}_{H,t} + \tilde{I}_{H,t} + \tilde{C}_t^g + \tilde{X}_t$$

$$Y_t = \tilde{C}_t + p_t^I\tilde{I}_t + p_t^H\tilde{C}_t^g + (p_t^H\tilde{X}_t - z_t\tilde{C}_F + z_t\tilde{I}_{F,t})$$

$$Y_t = p_t^H\tilde{Y}_t^H$$

$$\tilde{K}_t^Y = (1-\delta)\tilde{K}_{t-1}^Y\left(\frac{1}{g_t^A}\right)^{\frac{1}{1-\alpha_K-\alpha_g}} + \tilde{I}_t^K$$
$$- \frac{\psi_Y}{2}\left(\frac{\tilde{I}_t^K}{\tilde{K}_{t-1}^Y}(g_{t+1}^A)^{\frac{1}{1-\alpha_K-\alpha_g}} - \delta_Y\right)^2\tilde{K}_{t-1}^Y\left(\frac{1}{g_t^A}\right)^{\frac{1}{1-\alpha_K-\alpha_g}}$$

$$\tilde{W}_t N_t^d + p_t^I \tilde{I}_t^K = \sigma \left( Q_t \tilde{K}_{t-1}^Y \left( \frac{1}{g_t^A} \right)^{\frac{1}{1-\alpha_K-\alpha_g}} \right)$$

$$Q_t = \frac{p_t^I \left( (1-\tau_t^\pi) + \varsigma_t \right)}{\left( 1 - \psi_Y \left( \frac{\tilde{I}_t^K}{\tilde{K}_{t-1}^Y} \left( \frac{1}{g_t^A} \right)^{\frac{1}{1-\alpha_K-\alpha_g}} - \delta_Y \right) \right)}$$

$$\begin{aligned} Q_t = \beta \frac{\tilde{\Delta}_{t+1}^K}{\tilde{\Delta}_t^K} \left( \frac{1}{g_{t+1}^A} \right)^{\frac{1}{1-\alpha_K-\alpha_g}} & \left( (1-\tau_t^\pi) \alpha_K p_{t+1}^H \frac{\tilde{Y}_{t+1}^H}{\tilde{K}_t^Y} (g_{t+1}^A)^{\frac{1}{1-\alpha_K-\alpha_g}} \right. \\ + \quad Q_{t+1} & \left( (1-\delta) - \frac{\psi_Y}{2} \left( \frac{\tilde{I}_{t+1}^K}{\tilde{K}_t^Y} (g_{t+1}^A)^{\frac{1}{1-\alpha_K-\alpha_g}} - \delta_Y \right)^2 \right) + \\ & Q_{t+1} \frac{\psi_Y}{2} \left( \frac{\tilde{I}_{t+1}^K}{\tilde{K}_t^Y} (g_{t+1}^A)^{\frac{1}{1-\alpha_K-\alpha_g}} - \delta_Y \right)^2 \left. \frac{\tilde{I}_{t+1}^K}{\tilde{K}_t^Y} (g_{t+1}^A)^{\frac{1}{1-\alpha_K-\alpha_g}} + \varsigma_{t+1} \sigma \right) \end{aligned}$$

$$(1-\tau_t^\pi)(1-\alpha_K) p_t^H \frac{\tilde{Y}_t^H}{N_t^d} = (1+\varsigma_t) \tilde{W}_t$$

$$\tilde{\Pi}_t = p_t^H \tilde{Y}_t^H - \tilde{W}_t N_t^d - p_t^I \tilde{I}_t^K$$

$$\tilde{K}_t^{gr} = (1-\delta_{gr}) \tilde{K}_{t-1}^{gr} \left( \frac{1}{g_t^A} \right)^{\frac{1}{1-\alpha_K-\alpha_g}} + \varepsilon \tilde{I}_t^{gr}$$

$$\tilde{K}_t^{gn} = (1-\delta_{gn}(s)) \tilde{K}_{t-1}^{gn} \left( \frac{1}{g_t^A} \right)^{\frac{1}{1-\alpha_K-\alpha_g}} + \varepsilon \tilde{I}_t^{gn}$$

$$\tilde{K}_t^G = \tilde{K}_t^{gnr} + \tilde{K}_t^{gr}$$

$$\begin{aligned} \tau_t^C \tilde{C}_t + \tau_t^l \tilde{W}_t \tilde{N}_t^d + \tau_t^\pi \tilde{\Pi}_t + \tilde{T}_t^G + z_t \tilde{B}_t^G + z_t \tilde{T}_t^{G*} & \\ = p_t^H \tilde{C}_t^g + \tilde{T}_t^{GW} + p_t^I \tilde{I}_t^{gn} + p_t^{gr} \tilde{I}_t^{gr} + z_t R_{t-1}^* \tilde{B}_{t-1}^{G*} \left( \frac{1}{g_t^A} \right)^{\frac{1}{1-\alpha_K-\alpha_g}} & \end{aligned}$$

$$\tilde{T}_t^G = T^G - \phi_b \left( \frac{z_t \tilde{B}_t^{G*}}{\tilde{Y}_t} - \frac{z B^{G*}}{Y} \right)$$

$$\tilde{T}_t^{GW} = T^{GW}$$

$$\tilde{C}_t^g = \tilde{C}^g$$

$$\tilde{I}_t^{gn} = \tilde{I}^{gn}$$

$$\tilde{I}_t^{gr} = \tilde{I}^{gr}$$

$$\tilde{Y}_t^* = Y^*$$

$$\tilde{X}_t = \left( \frac{p_t^H}{z_t} \right)^{-\eta_X} Y_t^*$$

$$C_{m,t}^a = C_m^a$$

$$W_t^* = W^*$$

$$z_t = \frac{\left( p_t^H \tilde{X}_t - z_t \tilde{C}_{F,t} + z_t \tilde{I}_{F,t} \right) + \tilde{T}_t^{W*}(s)}{(\tilde{B}_t^* - \tilde{B}_t^{G*}) - R_{t-1}^* \left( \frac{1}{g_t^A} \right)^{\frac{1}{1-\alpha_K-\alpha_g}} (\tilde{B}_{t-1}^* - \tilde{B}_{t-1}^{G*})}$$

$$R_t^* = \bar{R}^* + \Omega_u \left( \exp \left( \frac{z_t (\tilde{B}_t^* - \tilde{B}_t^{G*})}{\tilde{Y}_t} - \frac{z(B^* - B^{G*})}{Y} \right) - 1 \right)$$

$$z_t^Y = \rho_z z_{t-1}^z + \varepsilon_t^z$$

$$g_t^A = \left( \frac{A_t}{A_{t-1}} \right)$$

$$g_t^A = (1 - \rho_{gA}) g^A + \rho_{gA} g_{t-1}^A + \varepsilon_t^{gA}$$

PUBLICATIONS

**Building Macroeconomic Resilience to Natural Disasters and Persistent Temperature Changes: The Case of Peru**

Working Paper No. WP/2025/144